In vitro T-cell activation

SKG or BALB/c T cells (3.0×10^4) were stimulated for 72 h with plate-bound anti-CD3 mAb (2C11) in the presence or absence of plate-bound anti-CD28 mAb in RPMI-1640 medium supplemented with 10% fetal calf serum and 50 μM 2-mercaptoethanol. Cells were also stimulated with TPA (1.4 ng ml^{-1}) and ionomycin (0.14 μM). KJ1.26$^+$ T cells from DO or DO.SKG mice were stimulated with ovalbumin (323–339) peptide in the presence of X-irradiated syngeneic spleen cells (10^5 cells) as antigen-presenting cells in 96-well round-bottomed plates. The incorporation of [^{3}H]thymidine by proliferating lymphocytes during the last 6 h of the culture was measured.

Immunoprecipitation and western blotting

Thymocytes or purified T cells (5×10^6) were incubated with anti-CD3 mAb (2C11) for 20 min, followed by cross-linking with antibody against Armenian hamster immunoglobulin (Jackson ImmunoResearch) (10 μg ml^{-1}) at 37 °C for the indicated duration. For immunoprecipitation, cells were lysed with RIPA buffer (0.5% Triton X-100, 20 mM Tris-HCl pH 7.5, 1 mM EDTA, 150 mM NaCl, 20 mM NaF, 1 mM Na_3VO_4) supplemented with protease inhibitors. The immune complexes were recovered by Protein A-conjugated Sepharose beads. For western blot analyses, cells were directly lysed by sample-loading buffer for SDS–polyacrylamide gel electrophoresis (SDS–PAGE) and immediately boiled for 4 min. Recovered immune complexes or total cell lysates were subjected to SDS–PAGE and transferred to poly(vinylidene difluoride) membranes, which were blotted with various antibodies after being blocked with PBS/5% BSA. Antibodies specific for the following proteins were used: ZAP-70 (Santa Cruz Biotech), TCR-ζ (Santa Cruz Biotech), LAT (Upstate Biotechnology), PLC-γ1 (Upstate Biotechnology), activated or total ERK1/2, SAPK/JNK and p38 MAP kinases (Cell Signalling Technology) or phosophotyrosine (4G10) (Upstate Biotechnology).

Calcium mobilization

Thymocytes or purified T cells were loaded with Fura-2 acetoxymethyl ester (Nacarai) for 30 min at 37 °C. Cells were then incubated with anti-CD3 mAb as described above, washed and resuspended with PBS. $CaCl_2$ was added to the samples 2 min before cross-linking cell surface-bound anti-CD3 mAb with anti-hamster antibody (Jackson ImmunoResearch). Fura-2 fluorescence was measured by a spectrofluorimeter (Nihon Bunkou).

Received 4 August; accepted 13 October 2003; doi:10.1038/nature02119.

1. Harris, E. D. *Rheumatoid Arthritis* (W. B. Saunders, Philadelphia, 1997).
2. Feldmann, M., Brennan, F. M. & Maini, R. N. Rheumatoid arthritis. *Cell* **85,** 307–310 (1996).
3. Firestein, G. F. in *Textbook of Rheumatology* 5th edn (eds Kelley, W. N., Ruddy, S., Harris, E. D. & Sledge, C. B.) 851–897 (W. B. Saunders, Philadelphia, 1997).
4. Marrack, P., Kappler, J. & Kotzin, B. L. Autoimmune disease: why and where it occurs. *Nature Med.* **7,** 899–905 (2001).
5. von Boehmer, H. *et al.* Thymic selection revisited: how essential is it? *Immunol. Rev.* **191,** 62–78 (2003).
6. Chan, A. C., Iwashima, M., Turck, C. W. & Weiss, A. ZAP-70: a 70 kd protein-tyrosine kinase that associates with the TCR zeta chain. *Cell* **71,** 649–662 (1992).
7. Sakaguchi, S. & Sakaguchi, N. Thymus and autoimmunity: capacity of the normal thymus to produce pathogenic self-reactive T cells and conditions required for their induction of autoimmune disease. *J. Exp. Med.* **172,** 537–545 (1990).
8. Itoh, M. *et al.* Thymus and autoimmunity: production of CD25$^+$ CD4$^+$ naturally anergic and suppressive T cells as a key function of the thymus in maintaining immunologic self-tolerance. *J. Immunol.* **162,** 5317–5326 (1999).
9. Negishi, I. *et al.* Essential role for ZAP-70 in both positive and negative selection of thymocytes. *Nature* **376,** 435–438 (1995).
10. van Oers, N. S. *et al.* The 21- and 23-kD forms of TCR zeta are generated by specific ITAM phosphorylations. *Nature Immunol.* **1,** 322–328 (2000).
11. Iwashima, M. *et al.* Sequential interactions of the TCR with two distinct cytoplasmic tyrosine kinases. *Science* **263,** 1136–1139 (1994).
12. Zhang, W., Sloan-Lancaster, J., Kitchen, J., Trible, R. P. & Samelson, L. E. LAT: the ZAP-70 tyrosine kinase substrate that links T cell receptor to cellular activation. *Cell* **92,** 83–92 (1998).
13. Rincon, M. MAP-kinase signaling pathway in T cells. *Curr. Opin. Immunol.* **13,** 339–345 (2001).
14. Noraz, N. *et al.* Alternative antigen receptor (TCR) signaling in T cells derived from ZAP-70-deficient patients expressing high levels of Syk. *J. Biol. Chem.* **275,** 15832–15838 (2000).
15. Murphy, K. M., Heimberger, A. B. & Loh, D. Y. Induction by antigen of intrathymic apoptosis of CD4$^+$CD8$^+$TCR^{lo} thymocytes *in vivo*. *Science* **250,** 1720–1723 (1990).
16. Kisielow, P., Bluthmann, H., Staerz, U. D., Steinmetz, M. & von Boehmer, H. Tolerance in T-cell-receptor transgenic mice involves deletion of nonmature CD4$^+$8$^+$ thymocytes. *Nature* **333,** 742–746 (1988).
17. Kisielow, P., Teh, H. S., Bluthmann, H. & von Boehmer, H. Positive selection of antigen-specific T cells in thymus by restricting MHC molecules. *Nature* **335,** 730–733 (1988).
18. Wiest, D. L. *et al.* A spontaneously arising mutation in the DLAARN motif of murine ZAP-70 abrogates kinase activity and arrests thymocyte development. *Immunity* **6,** 663–671 (1997).
19. Sakaguchi, S., Sakaguchi, N., Asano, M., Itoh, M. & Toda, M. Immunologic self-tolerance maintained by activated T cells expressing IL-2 receptor α-chains (CD25). Breakdown of a single mechanism of self-tolerance causes various autoimmune diseases. *J. Immunol.* **155,** 1151–1164 (1995).
20. Keffer, J. *et al.* Transgenic mice expressing human tumor necrosis factor: a predictive genetic model of arthritis. *EMBO J.* **10,** 4025–4031 (1991).
21. Kouskoff, V. *et al.* Organ-specific disease provoked by systemic autoimmunity. *Cell* **87,** 811–822 (1996).
22. Pals, S. T., Radaszkiewicz, T., Roozendaal, L. & Gleichman, E. Chronic progressive polyarthritis and other symptoms of collagen vascular disease induced by graft-versus-host reaction. *J. Immunol.* **134,** 1475–1482 (1985).
23. Nishimura, H., Nose, M., Hiai, H., Minato, N. & Honjo, T. Development of lupus-like autoimmune diseases by disruption of the PD-1 gene encoding an ITIM motif-carrying immunoreceptor. *Immunity* **11,** 141–151 (1999).
24. Horai, R. *et al.* Development of chronic inflammatory arthropathy resembling rheumatoid arthritis in interleukin 1 receptor antagonist-deficient mice. *J. Exp. Med.* **191,** 313–320 (2000).
25. Atsumi, T. *et al.* A point mutation of Tyr-759 in interleukin 6 family cytokine receptor subunit gp130 causes autoimmune arthritis. *J. Exp. Med.* **196,** 979–990 (2002).
26. Dayer, J. M. & Burger, D. Cytokines and direct cell contact in synovitis: relevance to therapeutic intervention. *Arthritis Res.* **1,** 17–20 (1999).
27. Naka, T., Nishimoto, N. & Kishimoto, T. The paradigm of IL-6: from basic science to medicine. *Arthritis Res.* **4** (Suppl. 3), S233–S242 (2002).
28. Werlen, G., Hausmann, B., Naeher, D. & Palmer, E. Signaling life and death in the thymus: timing is everything. *Science* **299,** 1859–1863 (2003).
29. Nambiar, M. P. *et al.* T cell signalling abnormalities in systemic lupus erythematosus are associated with increased mutations/polymorphisms and splice variants of T cell receptor zeta chain messenger RNA. *Arthritis Rheum.* **44,** 1336–1350 (2001).
30. Takeuchi, T. *et al.* TCR zeta chain lacking exon 7 in two patients with systemic lupus erythematosus. *Int. Immunol.* **10,** 911–921 (1998).

Supplementary Information accompanies the paper on **www.nature.com/nature**.

Acknowledgements We thank H. von Boemer for transgenic mice; M. Singh (GBF, Germany) for a gift of recombinant HSP-70 through the support of the UNDP/World Bank/WHO Special Program for Research and Training on Tropical Diseases; F. Melchers, R. Zinkernagel, K. Yamamoto, R. Suzuki and Z. Fehervari for discussion; A. Kosugi and T. Nakayama for reagents; and E. Moriizumi for immunohistochemistry and histology. This work was supported by grants-in-aid from the Ministry of Education, Science, Sports and Culture, the Ministry of Human Welfare, Japan Science and Technology Corporation, and the Organization for Pharmaceutical Safety and Research of Japan.

Authors' contributions The SKG strain was established by S.S. and N.S. The experiments in Figs 1, 2a–d, 3f–h, 4, Supplementary Figs 1, 4 and 6 were conducted by N.S. and S.S.; those in Fig. 2b–d by Ta.T., N.S., H.H., To.T., S.Y., T. S., S.N. and S.S.; those in Figs 2e, f, 3a–c, e and Supplementary Fig. 2 by Ta.T.; that in Fig. 3d by To.T.; that in Supplementary Fig. 3 by T.N., and that in Supplementary Fig. 5 by T.M. ZAP-70-deficient mice were provided by I.N.

Competing interests statement The authors declare that they have no competing financial interests.

Correspondence and requests for materials should be addressed to S.S. (shimon@frontier.kyoto-u.ac.jp).

A positive-feedback-based bistable 'memory module' that governs a cell fate decision

Wen Xiong & James E. Ferrell Jr

Department of Molecular Pharmacology, Stanford University School of Medicine, Stanford, California 94305-5174, USA

The maturation of *Xenopus* oocytes can be thought of as a process of cell fate induction, with the immature oocyte representing the default fate and the mature oocyte representing the induced fate[1,2]. Crucial mediators of *Xenopus* oocyte maturation, including the p42 mitogen-activated protein kinase (MAPK) and the cell-division cycle protein kinase Cdc2, are known to be organized into positive feedback loops[3]. In principle, such positive feedback loops could produce an actively maintained 'memory' of a transient inductive stimulus and could explain the irreversibility of maturation[3–6]. Here we show that the p42 MAPK and Cdc2 system normally generates an irreversible biochemical response from a transient stimulus, but the response becomes transient when positive feedback is blocked. Our results explain how a group of intrinsically reversible signal transducers can generate an irreversible response at a systems level, and show how a cell fate can be maintained by a self-sustaining pattern of protein kinase activation.

Immature *Xenopus* oocytes are arrested in a G2-like phase of the cell cycle. In response to steroid hormones, the oocyte is released

from its G2 arrest, undergoes germinal vesicle breakdown (GVBD), completes meiosis I, proceeds directly into meiosis II, and then arrests again in the metaphase of meiosis II. Early work indicated that at some point in this process, the oocyte irrevocably commits to maturation[7–9]. We corroborated these observations by using low concentrations of the steroid hormone progesterone and thorough washing procedures to minimize the possibility that commitment was an artefact of inadequate washing. We found that oocytes generally committed to maturation after 2–4 h of progesterone treatment and before (and in one experiment just before) GVBD (Fig. 1a–c). This timing agrees well with studies of the acquisition of 'maturation inertia' in *Rana temporaria* oocytes treated with gonadotropin[7]. Oocytes remained arrested in their mature, GVBD state for up to several days after progesterone removal. Thus, transient treatment with progesterone results in a sustained cellular response.

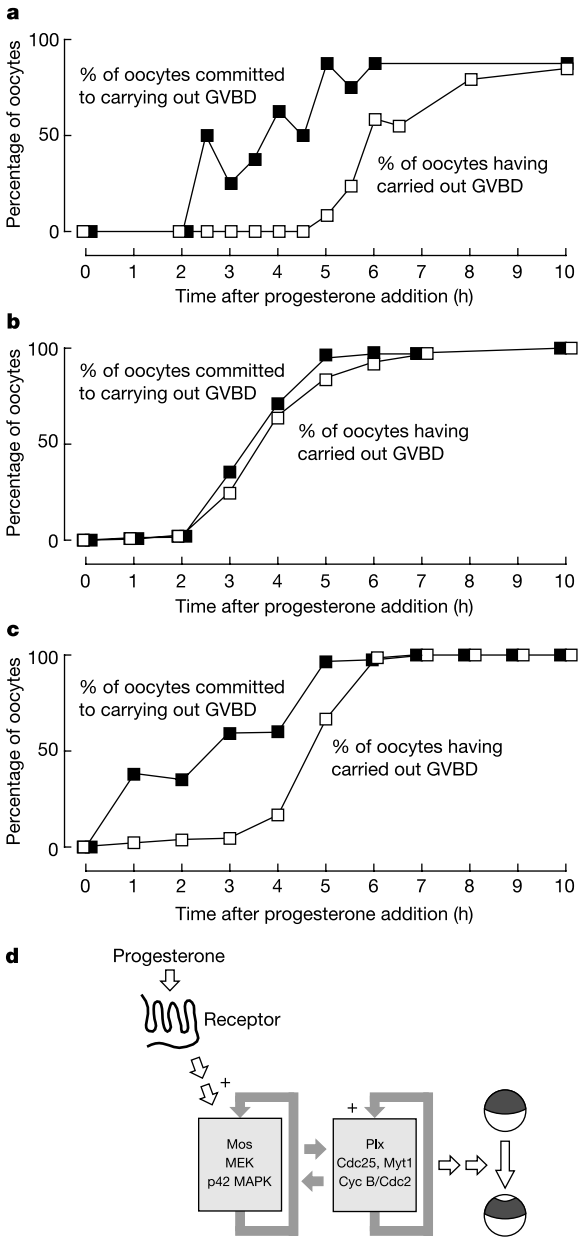

Figure 1 Cell fate commitment during oocyte maturation. **a**–**c**, Timing of commitment versus maturation from three independent experiments. **d**, View of the signal transduction network that culminates in *Xenopus* oocyte maturation.

At a biochemical level, oocyte maturation is controlled by p42 MAPK and cyclin B/Cdc2 (Fig. 1d). Both of these protein kinases are activated during maturation: p42 MAPK through phosphorylation by MAPK kinase (MEK), and cyclin B/Cdc2 through dephosphorylation by Cdc25. In addition, both kinases seem to be actively maintained in their high-activity, M-phase states. For example, in mature oocytes where p42 MAPK activity is high and unchanging, the two phosphorylation events that activate p42 MAPK still turn over rapidly with half-lives ($t_{1/2}$) of about 5 min (ref. 10). EDTA-quenching experiments suggest that phosphorylation events turn over rapidly ($t_{1/2} < 10$ min) in other members of the MAPK cascade, Mos and MEK, and also in Cdc25 and Wee1 (data not shown). This raises the issue of how these intrinsically reversible signalling proteins can 'remember' a transient stimulus and convert it into an irreversible response.

An attractive possibility is that the irreversibility is produced by positive feedback, and indeed numerous positive feedback loops have been identified in the p42 MAPK/Cdc2 network of an oocyte. For example, Mos activates p42 MAPK through the intermediacy of MEK, and active p42 MAPK feeds back to promote the accumulation of Mos (refs 11–13 and Fig. 1d). This protein-synthesis-dependent positive feedback loop is strong enough to allow p42 MAPK to show an all-or-none, bistable response to progesterone or microinjected Mos[14]. If protein synthesis is blocked (and thus the positive feedback is blocked), however, the response becomes graded[14].

Other positive feedback loops are also present in the signalling network that culminates in oocyte maturation. Cdc2 promotes activation of the Cdc2 activator Cdc25 (refs 15, 16), and promotes inactivation of the Cdc2 inhibitor Myt1 (ref. 17 and Fig. 1d). The p42 MAPK and Cdc2 systems also interact with each other through positive feedback: p42 MAPK acts positively on Cdc2 by promoting the inactivation of Myt1 (ref. 18), and Cdc2 acts positively on p42 MAPK by promoting the accumulation of Mos (ref. 19 and Fig. 1d). Thus, positive feedback is a recurring theme in oocyte signal transduction, and indeed positive feedback and bistability are important in various biological contexts[20–23].

In theory, a system whose positive feedback is strong enough to produce bistability should show either hysteresis (meaning that it is easier to maintain the system in its on state than to toggle the system from off to on) or, if the feedback is particularly strong, irreversibility (Box 1). We considered that the bistable p42 MAPK/Cdc2 system of the oocyte might possess sufficiently strong positive feedback to allow the system to generate this type of self-sustaining, actively maintained irreversibility.

To test this hypothesis, we set out to determine whether hysteresis or irreversibility is apparent in the oocyte's response to progesterone. This amounts to determining whether the concentration of progesterone needed to induce p42 MAPK phosphorylation and Cdc2 activation differs from that needed to maintain the activities of these kinases. To obtain 'induction' stimulus–response curves, we incubated immature oocytes with different concentrations of progesterone, waited until oocyte maturation had reached a plateau, and then measured the percentage of GVBD (%GVBD), p42 MAPK phosphorylation, Cdc2 activation and progesterone binding. Progesterone-treated oocytes showed dose-dependent increases in all of these responses (Fig. 2a–c, 'induction'), with maximal kinase activation and %GVBD obtained with 600 nM progesterone.

To obtain 'maintenance' stimulus–response curves, we incubated oocytes with 600 nM progesterone, waited until GVBD had reached a plateau (5 h in the experiments shown in Fig. 2), washed the oocytes for 10 h to remove progesterone, and then resuspended the washed oocytes in various concentrations of progesterone. After 5 h of further incubation, we monitored %GVBD, p42 MAPK phosphorylation, Cdc2 activation and progesterone binding. Oocytes were found to maintain maximal p42 MAPK and Cdc2 activities after being washed free of progesterone (Fig. 2b, c, 'maintenance'),

and none of the oocytes lost its white dot (Fig. 2a). The progesterone-binding data argued against the trivial explanation that the irreversibility in the p42 MAPK and Cdc2 responses was simply due to a failure to wash the progesterone away adequately (Fig. 2d). Thus, once oocytes are mature, the continued presence of progesterone seems to be unnecessary. Some 'memory' of the progesterone must be maintained either by the p42 MAPK/Cdc2 system or by signal transducers upstream of this system.

To test whether the p42 MAPK/Cdc2 system itself can generate an irreversible response from a transient stimulus, we used a chimaeric protein of Raf and the oestrogen receptor (ΔRaf:ER), in which an activated Raf1 protein is rendered conditional by fusion to an ER hormone-binding domain[24]. In oocytes expressing ΔRaf:ER, the steroid hormone oestradiol (which by itself has no effect on maturation, p42 MAPK activation or Cdc2 activation in oocytes) can be used to introduce a stimulus directly into the MAPK cascade, bypassing the progesterone receptor and other upstream signalling proteins.

Oocytes expressing ΔRaf:ER possessed low but detectable ΔRaf:ER activity in the absence of oestradiol (Fig. 3a, middle, lane 3). In response to oestradiol, there was a prompt 3–5-fold increase in ΔRaf:ER activity (Fig. 3a, middle, lanes 3–5), followed by a slower, additional 3–5-fold increase in ΔRaf:ER protein and activity (Fig. 3a, top and middle, lanes 6–10). The MEK inhibitor PD98059 and the protein synthesis inhibitor cycloheximide blocked the slow increase in ΔRaf:ER protein (data not shown) and activity (Fig. 4a, c), indicating that this component of the ΔRaf:ER activation depends on positive feedback between p42 MAPK and ΔRaf:ER. Within several hours, the oestradiol-induced activation of ΔRaf:ER resulted in complete activation of endogenous p42 MAPK (Fig. 3a, bottom, lanes 9–10).

We used the ΔRaf:ER-expressing oocytes to look for hysteresis or irreversibility in the response to oestradiol, by using the induction versus maintenance strategy described above. When immature oocytes expressing ΔRaf:ER were treated with increasing concentrations of oestradiol, there was a graded, dose-dependent increase in %GVBD and in steady-state ΔRaf:ER activity, p42 MAPK phosphorylation and Cdc2 activity (Fig. 3b–e, 'induction'). The

Box 1

Behaviour of a simple positive feedback loop: sensitivity amplification, bistability, hysteresis and irreversibility

Positive feedback loops have the potential to convert a transient stimulus into a self-sustaining, irreversible response. But irreversibility is not an inevitable consequence of positive feedback, nor is irreversibility the only useful systems-level property that can emerge from systems with positive feedback loops. This is true in the case of complicated positive feedback systems, such as the p42 MAPK/Cdc2 system in oocytes, and is also true (and can be more easily seen and understood) in simpler systems, such as the one shown here (**a**).

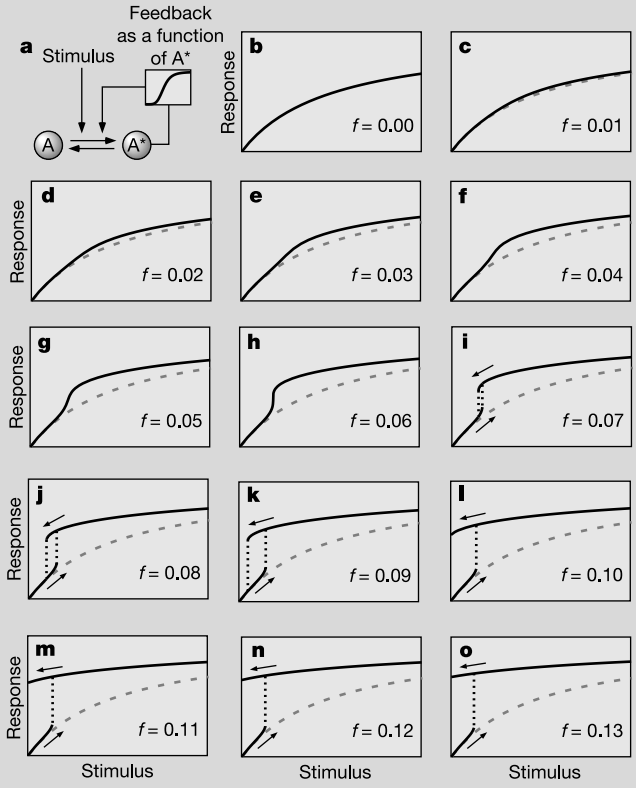

This system consists of a signalling protein that can be reversibly converted between an inactive form (A) and an active one (A*). The activation reaction is assumed to be regulated in two ways: by an external stimulus (equation (1), first term); and by positive feedback, with a nonlinear Hill equation relationship between the amount of A* produced and the rate of production of more A* (equation (1), second term). The inactivation reaction is assumed to be unregulated; its rate is proportional to the concentration of A* (equation (1), third term). Thus,

$$\frac{d[A^*]}{dt} = \{\text{stimulus} \times ([A_{tot}] - [A^*])\} + f\frac{[A^*]^n}{K^n + [A^*]^n} - k_{inact}[A^*] \qquad (1)$$

where n denotes the Hill coefficient, K is the effector concentration for half-maximum response (EC_{50}) for the feedback as a function of [A*], and f represents the strength of the feedback.

This differential equation was solved numerically (by using Mathematica 2.2.2) to determine the relationship between stimulus and steady-state response ([A*]), assuming that $n = 5$, $K = 1$, $k_{inact} = 0.01$ and stimulus = 0–1, and assuming a range of values of f. The results are shown in **b**–**o**, with the calculated steady-state responses shown as unbroken lines and the discontinuities shown as dotted lines; the no-feedback response (dashed lines) is included for comparison.

When $f = 0$, the response is monostable and the stimulus–response curve is a smooth michaelian hyperbola (**b**). As the strength of the feedback increases, the stimulus–response curve acquires a sigmoidal shape (**c**–**h**). This occurs because the feedback has been assumed to be cooperative or ultrasensitive. The sigmoidicity makes the response of A* more switch-like (but still monostable).

At $f = 0.07$ (**i**), the stimulus–response curve splits into two curves: one representing the amount of stimulus needed to induce the system to turn on, the other representing the amount of stimulus needed to maintain the system in its on state. At this point, the system becomes bistable for some values of stimulus (that is, there are two discrete, stable steady states for a single value of stimulus) and the system shows hysteresis, meaning that the dose–response relationship is a loop rather than a curve. The range of stimulus over which the system is bistable and the extent of the hysteresis both increase as f increases (**i**–**k**).

Eventually, the feedback becomes strong enough to maintain the system in the on state even when the stimulus is decreased to zero (**l**–**o**). At this point, the system may be able to convert a transient stimulus into an essentially irreversible response. But even in a system such as this, stochastic effects still have the potential to make the response reversible[29,30].

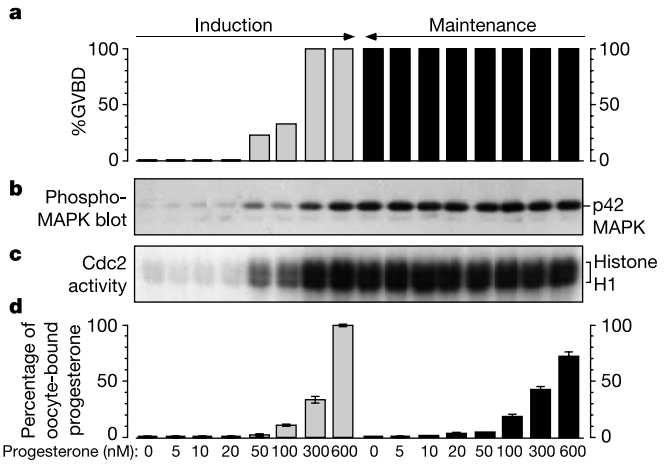

Figure 2 Irreversibility in the biochemical responses of oocytes to progesterone. GVBD (**a**), p42 MAPK phosphorylation (**b**), Cdc2 H1 kinase activity (**c**) and progesterone binding (**d**) were assessed at the end of the induction period and the end of the maintenance period. GVBD, MAPK phosphorylation and Cdc2 activity data are from one of three similar experiments. Progesterone binding data (shown as means ± s.d.) are from a separate experiment.

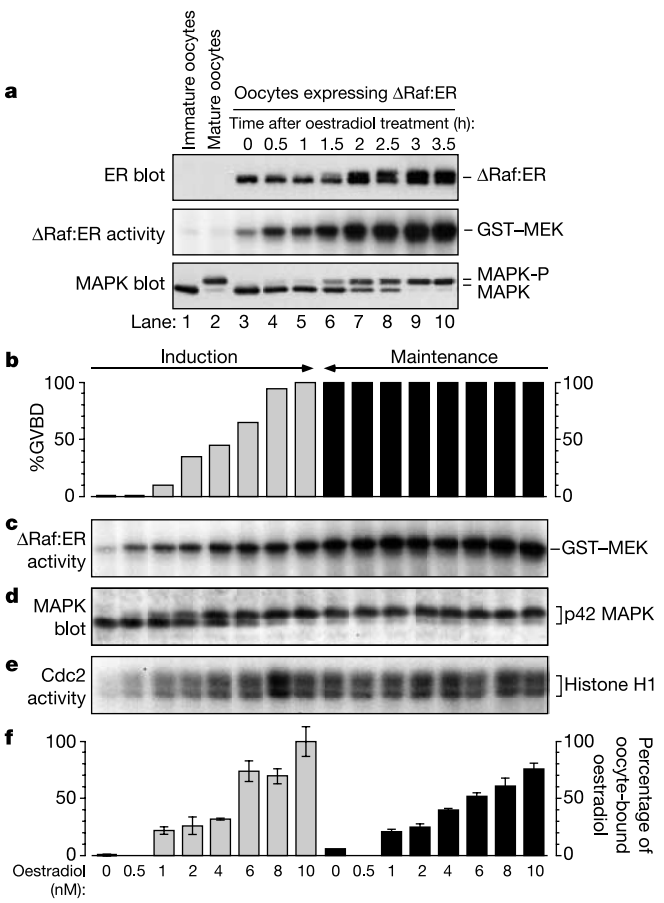

Figure 3 Irreversibility in the biochemical responses of oocytes expressing ΔRaf:ER to oestradiol. **a**, Time course of oestradiol-induced ΔRaf:ER and p42 MAPK activation, assessed by ER immunoblot analysis, ΔRaf:ER immune complex kinase assay, and p42 MAPK immunoblot analysis. **b**–**f**, Steady-state responses. GVBD (**b**), ΔRaf:ER activity (**c**), p42 MAPK phosphorylation (**d**), Cdc2 H1 kinase activity (**e**) and oestradiol binding (**f**) were assessed at the end of the induction period and the end of the maintenance period. GVBD, ΔRaf:ER activity, p42 MAPK phosphorylation and Cdc2 activity data are from one of three similar experiments. Oestradiol binding data (shown as means ± s.d.) are from a separate experiment.

kinases remained maximally active after the oestradiol was washed away (Fig. 3c–e, 'maintenance'), and every oocyte maintained its white spot after washing (Fig. 3b). The trivial explanation of incomplete removal of oestradiol did not seem to account for the observed irreversibility (Fig. 3f). Thus, the p42 MAPK/Cdc2 system itself can convert a transient stimulus into an irreversible activation response; that is, the system can generate a long-term 'memory' of a transient differentiation stimulus.

To determine whether positive feedback is essential for maintaining this memory, we made use of three ways of blocking feedback from p42 MAPK to Mos. The first feedback inhibitor was cycloheximide. If oocytes are provided with a sufficiently strong maturation stimulus, such as microinjected Mos or cyclin A, protein synthesis is not essential for maturation[25,26]; however, protein synthesis is essential for the feedback from p42 MAPK to Mos[11–13], and possibly for other interconnected positive feedback loops[27]. Thus, we examined whether cycloheximide would convert the observed irreversible oestradiol response into a reversible one. In the absence of cycloheximide, oestradiol again caused marked increases in the steady-state activities of ΔRaf:ER, p42 MAPK and Cdc2, and these responses were undiminished after washing (Fig. 4a). In the presence of cycloheximide, the responses of ΔRaf:ER and p42 MAPK to oestradiol were blunted, and the response of Cdc2 was markedly diminished (Fig. 4a). In addition, the responses were no longer irreversible: after the oestradiol was washed away, the activity of ΔRaf:ER, the phosphorylation of p42 MAPK, and the low activation of Cdc2 all decreased to near-basal levels (Fig. 4a). Thus, protein synthesis, which is essential for feedback from p42 MAPK to Mos, is also required for the irreversibility of the oestradiol responses.

The second feedback inhibitor was a morpholino Mos antisense oligonucleotide (Mos-AS), which blocks progesterone-induced Mos synthesis without globally abolishing protein synthesis[28]. Mos-AS blocked oestradiol-induced Mos synthesis and also abolished the irreversibility of ΔRaf:ER activation and p42 MAPK phosphorylation (Fig. 4b). The low Cdc2 activation induced by oestradiol also became reversible (Fig. 4b). Thus, Mos synthesis is required for the observed irreversibility. Finally, we examined the effects of the MEK inhibitor PD98059, which blocks both downstream effects and feedback effects that depend on MEK activation. PD98059 rendered oestradiol-induced ΔRaf:ER activation reversible and also blocked oestradiol-induced p42 MAPK and Cdc2 activation (Fig. 4c).

Taken together, these findings rule out the possibility that an inability to wash away ΔRaf:ER-bound oestradiol, or an intrinsic defect in the capacity of ΔRaf:ER to be inactivated, can account for the irreversible p42 MAPK and Cdc2 responses seen in Figs 3 and 4. Instead, the irreversibility seems to be actively generated by a bistable, positive feedback system, and compromising the feedback abolishes the irreversibility.

The idea that the irreversibility of the differentiated state might be maintained by feedback loops that generate self-sustaining patterns of gene expression dates back more than 40 years (ref. 4), and the recognition that feedback-enforced patterns of protein activity might also produce a systems-level 'memory' of transient stimuli dates back almost 20 years (ref. 5). Studies of artificial bistable gene expression systems in *Escherichia coli* and *Saccharomyces cerevisiae* have shown that bistable systems can in fact function as memory modules, but have also shown that stochastic effects sometimes cause two bistable steady states to equilibrate with each other, undermining any memory[29,30]. Our work provides experimental evidence that in a physiological process of cell fate induction, *Xenopus* oocyte maturation, a bistable signalling system

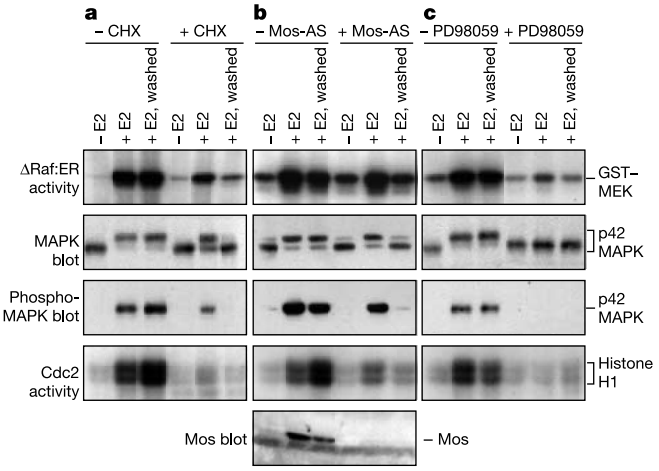

Figure 4 Positive feedback is required for irreversible biochemical responses. Oocytes expressing ΔRaf:ER were treated by an 18-h incubation with no added oestradiol (− E2); an 18-h incubation with 10 nM oestradiol (+ E2); or a 2-h incubation with 10 nM oestradiol, followed by a 16-h wash (+ E2, washed). **a**, A sample of oocytes was treated with cycloheximide (CHX, 100 μg ml^{-1}) to block protein synthesis and positive feedback. **b**, A sample of oocytes was injected with a morpholino Mos antisense oligonucleotide (100 ng per oocyte) to block Mos synthesis. **c**, A sample of oocytes was treated with the MEK inhibitor PD98059 (100 μM) to block MEK-mediated positive feedback and downstream events.

converts a transient stimulus into a reliable, self-sustaining, effectively irreversible pattern of protein activities. It will be interesting to see how common these bistable memory modules are in cell signalling. □

Methods

Oocytes, expression constructs and reagents

Xenopus laevis oocytes were defolliculated by collagenase treatment and stage VI oocytes were manually sorted. We prepared oocyte lysates as described[10].

The high-activity DD form of ΔRaf:ER (in pBabepuro3)[24] was a gift from M. McMahon and was subcloned into pSP64(polyA). ΔRaf:ER mRNA was transcribed *in vitro* using an Sp6 transcription kit (Ambion), and the RNA concentration was determined by gel electrophoresis and staining. ΔRaf:ER mRNA (5 ng) was microinjected with a Nanoinjector (Drummond Scientific), and oocytes were left for protein expression for 2 h before oestradiol was added. We purchased the Mos antisense morpholino oligonucleotide 5′-AAGGCATTGCTGTGTGACTCGCTGA-3′ (ref. 28) from Gene Tools LLC.

Oestradiol, progesterone and cycloheximide were from Sigma, and [^{3}H]oestradiol and [^{14}C]progesterone were from New England Nuclear. The MEK inhibitor PD98059 was from Calbiochem.

SDS–PAGE and immunoblotting

For most assays, samples were resolved by electrophoresis on 10% low-bis polyacrylamide gels (acrylamide:bisacrylamide 100:1). For the Cdc2/cyclin B histone H1 kinase assays, we used 12.5% polyacrylamide gels (acrylamide:bisacrylamide 29:1). Gels were transferred to poly(vinylidene difluoride) blotting membranes, which were then blocked with 3% nonfat milk in Tris-buffered saline (150 mM NaCl and 20 mM Tris; pH 7.6) and incubated for 2 h with a 1:1,000 dilution of one of the following primary antibodies: anti-MAPK (DC3, raised in our own laboratory), anti-phospho-MAPK (9106, New England Biolabs), anti-ER (SC-543, Santa Cruz Biotechnology) or a 1:500 dilution of anti-MoS (SC-86, Santa Cruz Biotechnology). Blots were washed three times with Tris-buffered saline plus 0.1% Tween 20 and probed with alkaline-phosphatase-conjugated secondary antibody for detection by CDP-Star (Tropix-Perkin Elmer). For reprobing, blots were stripped in 100 ml of stripping buffer (100 mM Tris-HCl, pH 7.4, 100 mM β-mercaptoethanol and 2% SDS) at 70 °C for 40 min.

Kinase assays

We prepared immune complexes of ΔRaf:ER by incubating cell lysate with 30 μl of protein-A–Sepharose (Sigma) pre-coated with 1 μl of anti-ER antibody (SC-543, Santa Cruz Biotechnology). The immunoprecipitates were washed once with lysis buffer and once with kinase buffer (20 mM HEPES, 10 mM $MgCl_2$ and 1 mM $MnCl_2$; pH 7.4). Raf kinase reactions were done at 30 °C for 30 min in 40 μl of kinase buffer with 1 mM dithiotheitol, 1 μM ATP and 10 μCi [γ-^{32}P]ATP (Amersham) with 50 ng of purified recombinant GST–MEK (UBI) as a substrate. The reaction was stopped by boiling in sample buffer and resolved by electrophoresis on a 10% 100:1 polyacrylamide gel.

For the histone H1 kinase assay, oocytes were lysed in a volume of 10 μl per oocyte, and 2 μl of cleared lysate was added to 8 μl of EB buffer (80 mM β-glycerophosphate, 20 mM EGTA and 15 mM $MgCl_2$; pH 7.3) and mixed with an equal volume (10 μl) of reaction mixture (6.73 μl of 2 × H1 kinase buffer, 0.02 μl of 0.2 mM ATP, 1.0 μl of 10 mg ml^{-1} histone H1, 2.0 μl of 100 μM protein kinase inhibitor (Santa Cruz Biotechnology) and 0.25 μl of 10 mCi ml^{-1} [γ-^{32}P]ATP). Reactions were carried out at 30 °C for 15 min and terminated by the addition of 6 × sample buffer (4 μl) followed by boiling.

Washing procedure and scintillation counting

Oocytes incubated with progesterone or oestradiol were washed free of the steroids by a series of ten 1-h washes in 50 ml of OR2 solution. For some experiments, cycloheximide or MEK inhibitor (PD98059) was included in both the incubation and the washing buffer. Pre- and post-wash binding of progesterone and oestradiol was determined by the inclusion of radiolabelled tracers ([^{14}C]progesterone, final specific activity 83 μCi μmol^{-1}, and [^{3}H]oestradiol, final specific activity 25,000 μCi μmol^{-1}) and quantified by scintillation counting.

Received 9 April; accepted 18 September 2003; doi:10.1038/nature02089.

1. Abrieu, A., Doree, M. & Fisher, D. The interplay between cyclin-B–Cdc2 kinase (MPF) and MAP kinase during maturation of oocytes. *J. Cell Sci.* **114,** 257–267 (2001).
2. Nebreda, A. R. & Ferby, I. Regulation of the meiotic cell cycle in oocytes. *Curr. Opin. Cell Biol.* **12,** 666–675 (2000).
3. Ferrell, J. E. Self-perpetuating states in signal transduction: positive feedback, double-negative feedback and bistability. *Curr. Opin. Cell Biol.* **14,** 140–148 (2002).
4. Monod, J. & Jacob, F. General conclusions: teleonomic mechanisms in cellular metabolism, growth, and differentiation. *Cold Spring Harb. Symp. Quant. Biol.* **26,** 389–401 (1961).
5. Lisman, J. E. A mechanism for memory storage insensitive to molecular turnover: a bistable autophosphorylating kinase. *Proc. Natl Acad. Sci. USA* **82,** 3055–3057 (1985).
6. Thomas, R. & Kaufman, M. Multistationarity, the basis of cell differentiation and memory. I. Structural conditions of multistationarity and other nontrivial behavior. *Chaos* **11,** 170–179 (2001).
7. Dettlaff, T. A. Action of actinomycin and puromycin upon frog oocyte maturation. *J. Embryol. Exp. Morphol.* **16,** 183–195 (1966).
8. Schuetz, A. W. Action of hormones on germinal vesicle breakdown in frog (*Rana pipiens*) oocytes. *J. Exp. Zool.* **166,** 347–354 (1967).
9. Smith, L. D., Ecker, R. E. & Subtelny, S. *In vitro* induction of physiological maturation in *Rana pipiens* oocytes removed from their ovarian follicles. *Dev. Biol.* **17,** 627–643 (1968).
10. Sohaskey, M. L. & Ferrell, J. E. Jr Distinct, constitutively active MAPK phosphatases function in *Xenopus* oocytes: implications for p42 MAPK regulation *in vivo*. *Mol. Biol. Cell* **10,** 3729–3743 (1999).
11. Matten, W. T., Copeland, T. D., Ahn, N. G. & Vande Woude, G. F. Positive feedback between MAP kinase and Mos during *Xenopus* oocyte maturation. *Dev. Biol.* **179,** 485–492 (1996).
12. Roy, L. M. *et al.* Mos proto-oncogene function during oocyte maturation in *Xenopus*. *Oncogene* **12,** 2203–2211 (1996).
13. Gotoh, Y., Masuyama, N., Dell, K., Shirakabe, K. & Nishida, E. Initiation of *Xenopus* oocyte maturation by activation of the mitogen-activated protein kinase cascade. *J. Biol. Chem.* **270,** 25898–25904 (1995).
14. Ferrell, J. E. Jr & Machleder, E. M. The biochemical basis of an all-or-none cell fate switch in *Xenopus* oocytes. *Science* **280,** 895–898 (1998).
15. Kumagai, A. & Dunphy, W. G. Regulation of the cdc25 protein during the cell cycle in *Xenopus* extracts. *Cell* **70,** 139–151 (1992).
16. Hoffmann, I., Clarke, P. R., Marcote, M. J., Karsenti, E. & Draetta, G. Phosphorylation and activation of human cdc25-C by cdc2–cyclin B and its involvement in the self-amplification of MPF at mitosis. *EMBO J.* **12,** 53–63 (1993).
17. Mueller, P. R., Coleman, T. R., Kumagai, A. & Dunphy, W. G. Myt1: a membrane-associated inhibitory kinase that phosphorylates Cdc2 on both threonine-14 and tyrosine-15. *Science* **270,** 86–90 (1995).
18. Palmer, A., Gavin, A. C. & Nebreda, A. R. A link between MAP kinase and p34^{cdc2}/cyclin B during oocyte maturation: p90^{rsk} phosphorylates and inactivates the p34^{cdc2} inhibitory kinase Myt1. *EMBO J.* **17,** 5037–5047 (1998).
19. Nebreda, A. R., Gannon, J. V. & Hunt, T. Newly synthesized protein(s) must associate with p34^{cdc2} to activate MAP kinase and MPF during progesterone-induced maturation of *Xenopus* oocytes. *EMBO J.* **14,** 5597–5607 (1995).
20. Bhalla, U. S., Ram, P. T. & Iyengar, R. MAP kinase phosphatase as a locus of flexibility in a mitogen-activated protein kinase signaling network. *Science* **297,** 1018–1023 (2002).
21. Sha, W. *et al.* Hysteresis drives cell-cycle transitions in *Xenopus laevis* egg extracts. *Proc. Natl Acad. Sci. USA* **100,** 975–980 (2003).
22. Pomerening, J. R., Sontag, E. D. & Ferrell, J. E. Jr Building a cell cycle oscillator: hysteresis and bistability in the activation of Cdc2. *Nature Cell Biol.* **5,** 346–351 (2003).
23. Bagowski, C. P. & Ferrell, J. E. Bistability in the JNK cascade. *Curr. Biol.* **11,** 1176–1182 (2001).
24. Bosch, E., Cherwinski, H., Peterson, D. & McMahon, M. Mutations of critical amino acids affect the biological and biochemical properties of oncogenic A-Raf and Raf-1. *Oncogene* **15,** 1021–1033 (1997).
25. Yew, N., Mellini, M. L. & Vande Woude, G. F. Meiotic initiation by the *mos* protein in Xenopus. *Nature* **355,** 649–652 (1992).
26. Roy, L. M. *et al.* Activation of p34^{cdc2} kinase by cyclin A. *J. Cell Biol.* **113,** 507–514 (1991).
27. Groisman, I., Jung, M.-Y., Sarkissian, M., Cao, Q. & Richter, J. D. Translational control of the embryonic cell cycle. *Cell* **109,** 473–483 (2002).
28. Dupre, A., Jessus, C., Ozon, R. & Haccard, O. Mos is not required for the initiation of meiotic maturation in *Xenopus* oocytes. *EMBO J.* **21,** 4026–4036 (2002).
29. Gardner, T. S., Cantor, C. R. & Collins, J. J. Construction of a genetic toggle switch in *Escherichia coli*. *Nature* **403,** 339–342 (2000).
30. Becskei, A., Seraphin, B. & Serrano, L. Positive feedback in eukaryotic gene networks: cell differentiation by graded to binary response conversion. *EMBO J.* **20,** 2528–2535 (2001).

Acknowledgements We thank M. McMahon for the ΔRaf:ER constructs, and K. Cimprich and members of the Ferrell laboratory for discussions and comments on the manuscript. This work was supported by a grant from the NIH.

Competing interests statement The authors declare that they have no competing financial interests.

Correspondence and requests for materials should be addressed to J.E.F. (james.ferrell@stanford.edu).

Structure and nucleic-acid binding of the *Drosophila* Argonaute 2 PAZ domain

Andreas Lingel*, Bernd Simon*, Elisa Izaurralde & Michael Sattler

European Molecular Biology Laboratory, Meyerhofstrasse 1, D-69117 Heidelberg, Germany

* These authors contributed equally to this work

RNA interference is a conserved mechanism that regulates gene expression in response to the presence of double-stranded (ds)RNAs[1,2]. The RNase III-like enzyme Dicer first cleaves dsRNA into 21–23-nucleotide small interfering RNAs (siRNAs)[3–6]. In the effector step, the multimeric RNA-induced silencing complex (RISC) identifies messenger RNAs homologous to the siRNAs and promotes their degradation[3,7]. The Argonaute 2 protein (Ago2) is a critical component of RISC[8,9]. Both Argonaute and Dicer family proteins contain a common PAZ domain whose function is unknown[10]. Here we present the three-dimensional nuclear magnetic resonance structure of the *Drosophila melanogaster* Ago2 PAZ domain. This domain adopts a nucleic-acid-binding fold that is stabilized by conserved hydrophobic residues. The nucleic-acid-binding patch is located in a cleft between the surface of a central β-barrel and a conserved module comprising strands β3, β4 and helix α3. Because critical structural residues and the binding surface are conserved, we suggest that PAZ domains in all members of the Argonaute and Dicer families adopt a similar fold with nucleic-acid binding function, and that this plays an important part in gene silencing.

Ago2 is a member of the PPD family of proteins (PAZ and Piwi domains), which are characterized by an amino-terminal PAZ domain (named after the Piwi, Argonaute and Zwille/Pinhead proteins) and a carboxy-terminal Piwi domain[10,11]. The PPD family comprises highly basic proteins with relative molecular masses of approximately 100,000 (M_r 100K) that are present in metazoa and fungi but not in budding yeast. Members of this protein family have essential roles in RNA interference (RNAi) and related gene-silencing processes in several organisms, and have also been implicated in cell-fate determination[12]. The molecular function of these proteins is unknown. The Piwi domain is highly conserved and exists also in prokaryotes[10]. The less conserved 110-residue PAZ domain has only been identified in eukaryotes[10]. It is found exclusively in the Argonaute and Dicer protein families.

The solution structure of the Ago2 PAZ domain (Fig. 1 and Table 1) comprises a central five-stranded open β-barrel (strands β1, β2, β5–β7), an N-terminal helical region (helices α1, α2) and a conserved approximately 35-residue module (comprising β3, β4 and α3) between strands β2 and β5. The N and C termini of the PAZ fold (residues 1–120) form a small antiparallel β-sheet (strands β0, β7) and thus are in close spatial proximity, as expected for an independent structural domain. Notably, the β5–β6 loop has an approximately 30-residue insertion in PAZ domains of the Dicer proteins (Supplementary Fig. S1), which could modulate their function. On the basis of nuclear magnetic resonance (NMR) relaxation measurements the PAZ domain is monomeric in solution (Supplementary Fig. S2).

The structure of the PAZ domain is stabilized by conserved hydrophobic residues, suggesting a similar fold for all members of the family. The hydrophobic core of the central β-barrel is formed by Ile 40, Val 42, Tyr 44, Tyr 57, Val 59, Leu 62, Leu 100, Val 102, Ile 109, Leu 111 and Ile 113. Hydrophobic side chains are conserved in the interface between the β3, β4, α3 module (Ile 81, Tyr 84, Phe 85, Tyr 90) and the central β-barrel (Tyr 44, Cys 99, Pro 112, Leu 115). The strands β6 and β7 and the connecting 3_{10} helix are highly conserved among PAZ domains (Supplementary Figs S1 and S3a). The 3_{10} helix contains the invariable Glu 114 residue, which contacts Tyr 90 and Phe 94 and is positioned to form a hydrogen bond with the Lys 93 backbone amide. This leads to tight packing between the α3–β5 loop and β6/β7, additionally stabilizing the PAZ domain fold. Consistently, a Glu 114 to Lys mutation yields insoluble protein upon expression in *Escherichia coli* (data not shown). In a genetic screen in *Caenorhabditis elegans*, worms deficient in RNAi were isolated in which the corresponding Glu was mutated to Lys in the Ago2 homologue RDE-1 (ref. 13). Our structural analysis suggests that this mutation probably destabilizes the fold of the PAZ domain, resulting in a non-functional RDE-1 protein.

A surface plot coloured by the degree of sequence conservation among PAZ domains (Fig. 2a) reveals a region comprising the β3, β4, α3 module and the central β-barrel, which together form a clamp-like structure (Figs 1b and 2a). The presence of aromatic and positively charged residues at this surface (Fig. 2b) may indicate a conserved function in the binding of negatively charged ligands, such as nucleic acids. A further hint at a potential role of PAZ domains in nucleic-acid binding comes from the five-stranded

Table 1 **Structural statistics for the Ago2 PAZ domain**

Statistics	⟨SA⟩*	⟨SA^{watref}⟩*
r.m.s. deviation (Å) from experimental distance restraints†		
Unambiguous/ambiguous (3,370/46)	0.0078 ± 0.0009	0.014 ± 0.001
Hydrogen bonds (18 × 2)	0.021 ± 0.002	0.042 ± 0.003
R.m.s. deviation (°) from experimental torsion restraints‡		
Dihedral angles (139 ϕ, 105 ψ)	0.44 ± 0.06	0.68 ± 0.1
R.m.s. deviation (Hz) from residual dipolar coupling restraints§		
H^N–N (32)	0.62 ± 0.09	1.00 ± 0.11
Coordinate precision (Å) residues 4–120‖		
N, Cα, C′ (secondary structure elements)	0.40 ± 0.04	0.51 ± 0.09
N, Cα, C′	0.49 ± 0.08	0.59 ± 0.08
All heavy atoms	0.94 ± 0.07	1.04 ± 0.06
Structural quality¶		
Bad contacts	2.3 ± 0.8	0.3 ± 0.5
Ramachandran plot		
Per cent in most favoured region	83.7 ± 1.9	89.9 ± 2.5
Per cent in additionally allowed region	14.8 ± 2.0	8.9 ± 2.5

* ⟨SA⟩ is an ensemble of ten lowest-energy solution structures of the Ago2 PAZ domain (out of 100 calculated). The CNS E_{repel} function was used to simulate van der Waals interactions with an energy constant of 25.0 kcal mol^{-1}Å^{-4} using 'PROLSQ' van der Waals radii. Root mean square (r.m.s.) deviations for bond lengths, bond angles and improper dihedral angles are 0.00156 ± 0.00004 Å, 0.327 ± 0.005° and 0.256 ± 0.014°, respectively. 1 kcal = 4.18 kJ. For ⟨SA^{watref}⟩, the ensemble of ⟨SA⟩ structures was refined in a shell of water as described[24].

† Distance restraints were used with a soft square-well potential using an energy constant of 50 kcal mol^{-1} Å^{-2}. For hydrogen bonds, distance restraints with bounds of 1.8–2.3 Å (H–O) and 2.8–3.3 Å (N–O) were derived for slow-exchanging amide protons. No distance restraint was violated by more than 0.3 Å in any of the final ⟨SA⟩ structures.

‡ Dihedral angle restraints, derived from $^3J(H^N,H\alpha)$ coupling constants and TALOS[21], were applied to ϕ and ψ using energy constants of 200 kcal mol^{-1} rad^{-2}. No dihedral angle restraint was violated by more than 5°.

§ Residual dipolar couplings were applied with a final energy constant of 0.3 kcal mol^{-1} Hz^{-2} for an alignment tensor with an axial component of 16.2 Hz and a rhombicity of 0.43.

‖ Coordinate precision is given as the cartesian coordinate r.m.s. deviation of the ten lowest-energy structures with respect to their mean structure.

¶ Structural quality was analysed using PROCHECK[25].

CORRIGENDUM

doi:10.1038/nature06125

A positive-feedback-based bistable 'memory module' that governs a cell fate decision

Wen Xiong & James E. Ferrell Jr

Nature 426, 460–465 (2003)

In Box 1, equation (1) should read

$$\frac{d[A^*]}{dt} = \{\text{stimulus} \times ([A_{tot}] - [A^*])\} + f\frac{[A^*]^n}{K^n + [A^*]^n}([A_{tot}] - [A^*]) - k_{inact}[A^*]$$

Setting $\frac{d[A^*]}{dt} = 0$, it follows that $\text{stimulus} = \frac{f \times [A^*]^n[A_{tot}] - k_{inact}K^n[A^*] - (f + k_{inact})[A^*]^{n+1}}{([A^*] - [A_{tot}])([A^*]^n + K^n)}$

which implicitly defines all of the possible steady state values of $[A^*]$ for any given value of the stimulus. The plots in Box 1 show only the stable steady states (the sections of the curves with positive slopes).

ERRATUM

doi:10.1038/nature06114

RNA-templated DNA repair

Francesca Storici, Katarzyna Bebenek, Thomas A. Kunkel, Dmitry A. Gordenin & Michael A. Resnick

Nature 447, 338–341 (2007)

In Figure 1, the column header indicating the repair frequencies should read "Repair frequency $(Leu^+) \times 10^{-7}$" rather than "Repair frequency $(Leu^+) \times 10^{-3}$ (per 10^7 viable cells)".

CORRIGENDUM

doi:10.1038/nature06169

Structure of the *E. coli* signal recognition particle bound to a translating ribosome

Christiane Schaffitzel, Miro Oswald, Imre Berger, Takashi Ishikawa, Jan Pieter Abrahams, Henk K. Koerten, Roman I. Koning & Nenad Ban

Nature 444, 503–506 (2006); doi:10.1038/nature05182 (published online 29 October 2006)

During the preparation of the manuscript, we inadvertently mislabelled ribosomal protein L32 as ribosomal protein L18 when interpreting the density based on the 50S coordinates (PDB accession number 2AW4). Therefore, whenever L18 is mentioned in the text and in Figs 3 and 4, it should be considered to refer to ribosomal protein L32. Our results and conclusions are not affected.